

ENHANCED MECHANICAL AND PHYSICAL PROPERTIES OF CONVENTIONAL GLASS IONOMER CEMENT BY ADDING ZIRCONIUM NANOPARTICLES

Muhammad Touheed Ul Hassan^{*1}, Memoona Sehar², Hamayoun Khan³, Jamil Memon⁴, Saba Naz⁵, Abdul Hameed Khan⁶, Kanwal Shaheen⁷, Muhammad Baqi Billah⁸

^{*1}Institute of Physics, The Islamia University of Bahawalpur

²Department of Physics, University of Central Punjab, Lahore

³Department of Chemistry, Abdul Wali Khan University, Mardan, Khyber Pakhtunkhwa, Pakistan

⁴Government College for Information Technology, Hala, Education and Literacy Department, Govt of Sindh, Pakistan

⁵Dr. M. A. Kazi Institute of Chemistry, University of Sindh, Jamshoro, Pakistan

⁶Department of Mechanical Engineering, University of Engineering Technology Mardan, Khyber Pakhtunkhwa, Pakistan

⁷Department of Chemistry, Comsats Institute of Technology Islamabad, Lahore campus, Pakistan

⁸School of Civil Engineering, Southeast University, China

^{*1}touheed8533@gmail.com, ²monasehar93@gmail.com, ³hamayounkhan795@gmail.com,

⁴jameelmemon2001@gmail.com, ⁵saba.naz@usindh.edu.pk, ⁶engrabdulhameed@uetmardan.edu.pk,

⁷kanwal123shaheen@gmail.com, ⁸baqibillah60@gmail.com

DOI: <https://doi.org/10.5281/zenodo.19059815>

Keywords

Glass ionomer cement, ZrO₂ nanoparticles, Mechanical properties

Article History

Received: 05 January 2026

Accepted: 18 February 2026

Published: 17 March 2026

Copyright @Author

Corresponding Author: *
Muhammad Touheed Ul
Hassan

Abstract

This study investigated the enhancement of the mechanical properties of conventional glass ionomer cement (GIC) through the incorporation of zirconium dioxide (ZrO₂) nanoparticles to overcome its inherent limitations in strength and durability. ZrO₂ nanoparticles were added at concentrations of 4%, 6%, and 8% to evaluate their effects on tensile strength, hardness, and structural resilience. Advanced characterization techniques were employed to examine the modified materials. X-ray diffraction (XRD) analysis assessed crystalline structure and phase composition, energy-dispersive X-ray spectroscopy (EDX) confirmed elemental composition and nanoparticle dispersion, Fourier-transform infrared (FTIR) spectroscopy identified chemical interactions between ZrO₂ and the GIC matrix, and scanning electron microscopy (SEM) evaluated microstructural changes. The results demonstrated a significant improvement in mechanical properties following nanoparticle incorporation, with the 6% ZrO₂ concentration exhibiting the highest Young's modulus during tensile testing. Enhanced stress tolerance and structural integrity suggested improved durability and potential longevity of dental restorations. Overall, the findings indicated that ZrO₂ nanoparticle reinforcement substantially improved GIC performance, highlighting the potential of nanotechnology in advancing restorative dental materials.

INTRODUCTION

1.1 Background

Dental caries remains one of the most prevalent chronic diseases worldwide and continues to be a major cause of oral pain and tooth loss across all age groups (Peres et al., 2019). The management of carious lesions typically involves the removal of infected tooth structure followed by restoration using suitable biomaterials. Although modern restorative dentistry offers a wide array of aesthetic and functional materials, the long-term success of tooth restorations remains a significant clinical challenge. Repeated replacement of restorations often results in progressive loss of sound tooth structure, initiating a restorative “cycle of re-intervention” that ultimately compromises tooth vitality and structural integrity (Hickel et al., 2007).

The most common causes of restoration failure include caries associated with restorations and sealants (CARS), marginal degradation, fracture of the restorative material, and loss of retention (Politis et al., 2016; Pani, 2022). Each replacement procedure increases the risk of further weakening the tooth, potentially leading to endodontic treatment or extraction. Consequently, contemporary restorative philosophy emphasizes minimally invasive dentistry and preservation of healthy tooth tissue (Leal et al., 2022).

An ideal restorative material should provide strong physical and chemical adhesion to enamel and dentine, prevent bacterial infiltration, exhibit adequate mechanical properties, and maintain dimensional stability under functional stresses. However, no currently available material fulfills all these criteria (de Oliveira et al., 2018). Among restorative materials, glass ionomer cements (GICs) have gained considerable attention due to their fluoride release, chemical adhesion to tooth structure, and biocompatibility (Santos & Dahi Taleghani, 2022). Despite these advantages, conventional GICs exhibit inherent limitations, including brittleness, low tensile and flexural strength, and limited wear resistance, restricting their use in high-stress-bearing areas.

To overcome these drawbacks, modifications such as high-viscosity GICs and resin-modified glass ionomer cements (RMGICs) were introduced. RMGICs incorporate hydrophilic monomers such as 2-

hydroxyethyl methacrylate (HEMA) to improve mechanical strength and reduce early moisture sensitivity (Culbertson, 2001). Although these improvements enhanced handling and mechanical performance, challenges related to long-term durability and fracture resistance persist.

1.2 Restoration Failure and Tooth Integrity

Restoration failure may arise from biological, mechanical, or aesthetic factors (Hickel et al., 2007). Biologically, CARS is frequently reported as the primary reason for replacement (Al-Tae, 2019). However, secondary caries is not merely a consequence of marginal gaps but is strongly influenced by patient-specific factors such as oral hygiene and cariogenic biofilm accumulation (Mount et al., 2016). In the absence of biofilm, secondary caries does not develop regardless of restoration quality (Leonard & Weber, 1970).

Mechanically, tooth fractures—including cusp fractures and cracked tooth syndrome—represent another major cause of failure (Kahler, 2008). The interaction between restorative materials and tooth biomechanics remains complex. Brittle restorative materials may not adequately absorb occlusal forces, leading to crack propagation and catastrophic failure (Geurtsen et al., 2003).

Minimally invasive management strategies such as the “5 Rs” concept—Review, Refurbish, Reseal, Repair, and Replace—have been proposed to extend restoration longevity and preserve tooth structure (Leal et al., 2022). Replacement should be considered only after conservative options have been evaluated, as repeated full replacement accelerates structural compromise (Meyenberg, 2013).

1.3 Materials for Restoring Failed Tooth-Restoration Complexes

1.3.1 Dental Amalgam

Dental amalgam has historically been valued for its durability and cost-effectiveness, particularly in stress-bearing restorations. Long-term clinical trials have demonstrated acceptable performance in Class I and II cavities (Sharif et al., 2014). However, amalgam lacks aesthetic appeal and demonstrates poor adhesion to tooth structures, often requiring extensive cavity preparation for mechanical retention

(Agnihotry et al., 2016). Environmental concerns and the demand for tooth-colored restorations have further reduced its use.

1.3.2 Composite Resins

Resin composites revolutionized restorative dentistry by enabling adhesive, minimally invasive procedures (Mahla, 2016). Advances in filler technology and bonding systems have improved their strength and aesthetics. Nevertheless, polymerization shrinkage, microleakage, and hydrolytic degradation remain concerns (Ferracane, 2011). Over time, water absorption and breakdown of polymer matrices compromise mechanical properties and interfacial stability (Holland & Davis, 2008).

1.3.3 Glass Ionomer Cements (GICs)

GICs are widely used in atraumatic restorative treatment (ART) due to their chemical adhesion and fluoride release (Pragathi, 2018). Adhesion occurs via an ion-exchange mechanism between carboxylate groups of polyalkenoic acid and calcium ions in hydroxyapatite. This chemical interaction creates an ion-exchange layer that contributes to marginal sealing and caries resistance (Santos & Dahi Taleghani, 2022).

However, conventional GICs exhibit low fracture toughness and limited flexural strength, making them susceptible to crack propagation in load-bearing areas (Xie et al., 2000). High-viscosity GICs demonstrated improved compressive strength due to higher powder-to-liquid ratios and enhanced cross-linking (Ching et al., 2018). Encapsulated systems have shown superior compressive strength compared to hand-mixed formulations due to reduced porosity and consistent mixing (Nomoto & McCabe, 2001). Resin-modified GICs (RMGICs) further enhanced mechanical properties by incorporating resin components, thereby improving toughness and moisture resistance (Culbertson, 2001). Despite these improvements, long-term degradation and mechanical limitations remain areas of concern.

1.4 Liquid Component and Polyacid Chemistry

The liquid component of GICs typically consists of polyacrylic acid or its copolymers. Molecular weight and concentration of polyacids significantly influence viscosity, setting kinetics, and mechanical

strength (Smith, 1998). The addition of tartaric acid improves working time and compressive strength by regulating cation availability during the setting reaction (Sarbjajna et al., 2017).

Innovations in polyacid modification, including incorporation of biocompatible monomers such as N-vinyl pyrrolidone (NVP), have been investigated to enhance flexibility and salt bridge formation within the matrix (Piepenbrock et al., 2010). These modifications aim to improve adhesive and mechanical performance while maintaining biocompatibility.

1.5 Mechanical Properties and Adhesion

Mechanical properties such as compressive strength, flexural strength, fracture toughness, and microhardness are critical indicators of restorative performance (Chaitra, 2018). Although compressive strength is commonly reported, brittle materials like GICs are more susceptible to tensile stress-induced failure (Xie et al., 2000). Flexural strength testing is therefore considered a more reliable indicator of clinical durability.

Surface hardness, often measured using Knoop or Vickers hardness tests, reflects resistance to surface deformation and wear (Nguyen et al., 2019). Bond strength testing—either shear or tensile—evaluates adhesive performance at the tooth-restoration interface. Adhesion of GICs involves both micromechanical interlocking and ionic bonding with hydroxyapatite, forming a durable ion-exchange layer.

Despite advancements, achieving optimal mechanical resilience without compromising adhesion and fluoride release remains a central challenge in GIC development.

1.6 Rationale for the Present Study

Given the limitations of conventional and resin-modified GICs, there is a compelling need to enhance their mechanical performance while preserving their therapeutic benefits. Modifications at the material chemistry level—particularly within the resin matrix and polyacid components—may offer improved fracture resistance, bonding stability, and long-term durability.

Therefore, this study aimed to design and evaluate modified glass ionomer formulations with enhanced

physical and adhesive properties. By investigating mechanical performance, microstructural characteristics, and bonding behavior, this research sought to contribute to the development of advanced restorative materials capable of improving clinical longevity and minimizing restorative failure.

2. Methodology

2.1 Materials

A commercially available restorative cement matrix and nano-sized reinforcing particles were used for the preparation of composite samples. Additional supporting materials included a curing agent and a volatile diluent to facilitate uniform dispersion and handling of the mixture. Laboratory apparatus such as weighing balance, mixing equipment, molds, heating units, and sample containers were used for sample preparation and processing.

2.2 Preparation of Composite Samples

Composite specimens were prepared by incorporating nano-scale reinforcement particles into the base cement matrix at different weight percentages. The base material was obtained in powdered form and mixed with reinforcing nanoparticles at three different concentrations: 4 wt%, 6 wt%, and 8 wt%. A precision digital balance

was used to measure the required amounts of each component.

The powdered components were first blended thoroughly using a mechanical mixing system to ensure homogeneous distribution of nanoparticles within the matrix. After achieving uniform mixing, a curing medium was added in a fixed ratio to initiate the setting process and improve the consistency of the blend. A small amount of volatile medium was introduced to enhance dispersion and reduce agglomeration of nanoparticles.

The prepared mixtures were molded into standardized specimen shapes suitable for mechanical testing. After molding, the samples were allowed to set at ambient laboratory conditions for 24 hours to ensure complete curing. Subsequently, the samples were placed in a controlled oven at moderate temperature for further drying and stabilization. The prepared specimens were then stored in sealed containers for characterization and mechanical testing.

2.3 Sample Composition

Three different composite formulations were prepared based on the percentage of nanoparticle reinforcement incorporated into the base matrix.

Table 2.1
Composition of prepared composite samples

Sample	Matrix Material	Nanoparticle Content	Weight Percentage
S1	Base cement matrix	Reinforcement nanoparticles	4 wt%
S2	Base cement matrix	Reinforcement nanoparticles	6 wt%
S3	Base cement matrix	Reinforcement nanoparticles	8 wt%

2.4 Preparation of Test Specimens

To evaluate the mechanical performance of the composites, standardized specimens were fabricated in a dog-bone shape according to commonly used mechanical testing protocols. The powder mixture of the matrix and reinforcing nanoparticles was weighed accurately using an analytical balance and mixed thoroughly to achieve uniform particle distribution.

The blended powder was then combined with the curing medium using a controlled ratio and stirred until a workable consistency was obtained. The mixture was transferred into molds designed to produce dog-bone shaped specimens. The filled molds were left undisturbed at room temperature to allow the material to solidify completely.

After the curing period, the molded specimens were carefully removed and subjected to mild heating in a laboratory oven to remove residual moisture and

improve structural stability. The prepared specimens were then polished and stored prior to characterization and mechanical testing. In addition to mechanical testing samples, a portion of the material was finely ground using a mortar and pestle for structural and compositional analyses.

2.5 Characterization Techniques

Material characterization was carried out using several analytical techniques to investigate the structural, morphological, elemental, and mechanical properties of the prepared composites. These techniques provide valuable information about the behavior of materials at micro- and nano-scale levels and are widely used in materials science research (Janssens et al., 2017).

The characterization techniques used in this study include: X-ray Diffraction (XRD), Fourier Transform Infrared Spectroscopy (FTIR), Energy Dispersive X-ray Spectroscopy (EDX), Scanning Electron Microscopy (SEM), and Universal Testing Machine (UTM).

These analytical methods enabled the investigation of crystal structure, functional groups, surface morphology, elemental composition, and mechanical strength of the synthesized composites.

2.6 X-Ray Diffraction Analysis

X-ray diffraction (XRD) is a widely used technique for identifying crystalline phases and evaluating the structural properties of materials. The technique operates on the principle of diffraction of X-rays when they interact with the atomic planes of crystalline structures. The diffraction patterns obtained provide information regarding crystal structure, crystallite size, and lattice parameters (Warren, 1941).

In this study, XRD analysis was performed to determine the crystallinity and structural characteristics of the prepared composites. The diffraction patterns obtained were compared with standard reference data to identify the structural phases present in the samples. Particle size estimation was also performed using established crystallographic relationships.

2.7 Fourier Transform Infrared Spectroscopy

Fourier Transform Infrared Spectroscopy (FTIR) is a powerful analytical technique used to identify

functional groups and chemical bonding within materials. It measures the absorption of infrared radiation by molecular bonds at specific frequencies corresponding to vibrational energy levels (Shurvell, 2006).

FTIR analysis was performed to investigate the bonding interactions and structural changes occurring in the composite materials after the incorporation of reinforcing nanoparticles. The resulting spectra provided valuable information regarding molecular interactions and the presence of characteristic functional groups within the samples.

2.8 Energy Dispersive X-Ray Spectroscopy

Energy Dispersive X-ray Spectroscopy (EDX) is an elemental analysis technique commonly coupled with electron microscopy. It enables the identification and quantification of elements present in a material by measuring the characteristic X-rays emitted when the sample is bombarded with high-energy electrons.

In this study, EDX analysis was conducted to confirm the elemental composition of the synthesized composites and verify the successful incorporation of reinforcing nanoparticles within the matrix.

2.9 Scanning Electron Microscopy

Scanning Electron Microscopy (SEM) was used to examine the surface morphology and microstructural features of the prepared composite samples. SEM utilizes a focused electron beam that interacts with the surface of the sample, producing signals that generate high-resolution images of the material (Goldstein et al., 2018).

The technique was employed to observe the distribution of nanoparticles within the matrix and to analyze the surface characteristics of the synthesized composites.

2.10 Mechanical Testing Using Universal Testing Machine

The mechanical performance of the prepared composites was evaluated using a Universal Testing Machine (UTM). This instrument applies controlled mechanical forces such as tensile or compressive loads to determine properties including tensile strength, elongation, and elastic modulus.



The prepared dog-bone shaped specimens were mounted in the testing machine, and tensile tests were performed under controlled loading conditions. The data obtained from these tests were used to compare the mechanical behavior of composite samples with different nanoparticle concentrations.

3. Results and Discussion

3.1. FTIR Analysis

The FTIR spectra were recorded using KBr discs, spanning the 300-4000 cm^{-1} range. Figure 1 presents the infrared spectra for both the GIC and Zirconium dopant samples. In Figure 1(a), it can be observed that the hydroxyl peaks in the 3330-3360 cm^{-1} region are less prominent. A notable peak at 2930 cm^{-1} corresponds to the stretching vibrations of hydroxyl ions within the crystal network of GIC (Foroughi et al., 2016). Additionally, a peak at 1610 cm^{-1} is attributed to the (COOH) functional group in GIC, which appears relatively weak in the GIC powder spectrum. In Figures 1(b), 1(c), and 1(d), the bands in the 1000-1050 cm^{-1} range are linked to the vibrations of zirconium dioxide, while the broad

peak in the 3400-3450 cm^{-1} range signifies the presence of the OH group originating from the precursor intermediate (Zr-OH), associated with its stretching vibration mode. Furthermore, a curved peak at 1470-1503 cm^{-1} indicates the presence of C-H (alkanes). In the 1000-650 cm^{-1} range, strong peaks associated with C=C bending and C-I stretching groups of alkenes and halo compounds are observed. Moreover, the band observed at 2920-2930 cm^{-1} is associated with the vibration of aromatic protons and the stretching motions of C-H within the alkane group in the zirconium-doped GIC (Sahmetlioglu et al., 2006). Additionally, the peaks at 601, 593, 547, and 493 cm^{-1} are linked to the bending vibrations of phosphate groups. This suggests that zirconium has been incorporated into the GIC matrix, which may enhance both its mechanical properties and adhesion. The peak observed at 1025 cm^{-1} corresponds to the stretching motions of C-H in the alkane group, indicating various interactions between the GIC and the dopant samples.

Table 3.1: Different Functional groups and their strengths

Wavenumber (cm^{-1})	Bonding	Strength
1700	C=O stretch	S
1635	O-H stretch	M
630-400	Phosphate -bonding	M
601	ZrO ₂ - bond	M
1525	N-H deformation	S
1320	C-O stretch	M
1720	C=O stretch	S
1635	C=C stretch	W
1249	C-O stretch	M
1300	C-O stretch	M
1240	N-H deformation	S
1000	Si-O stretch	S

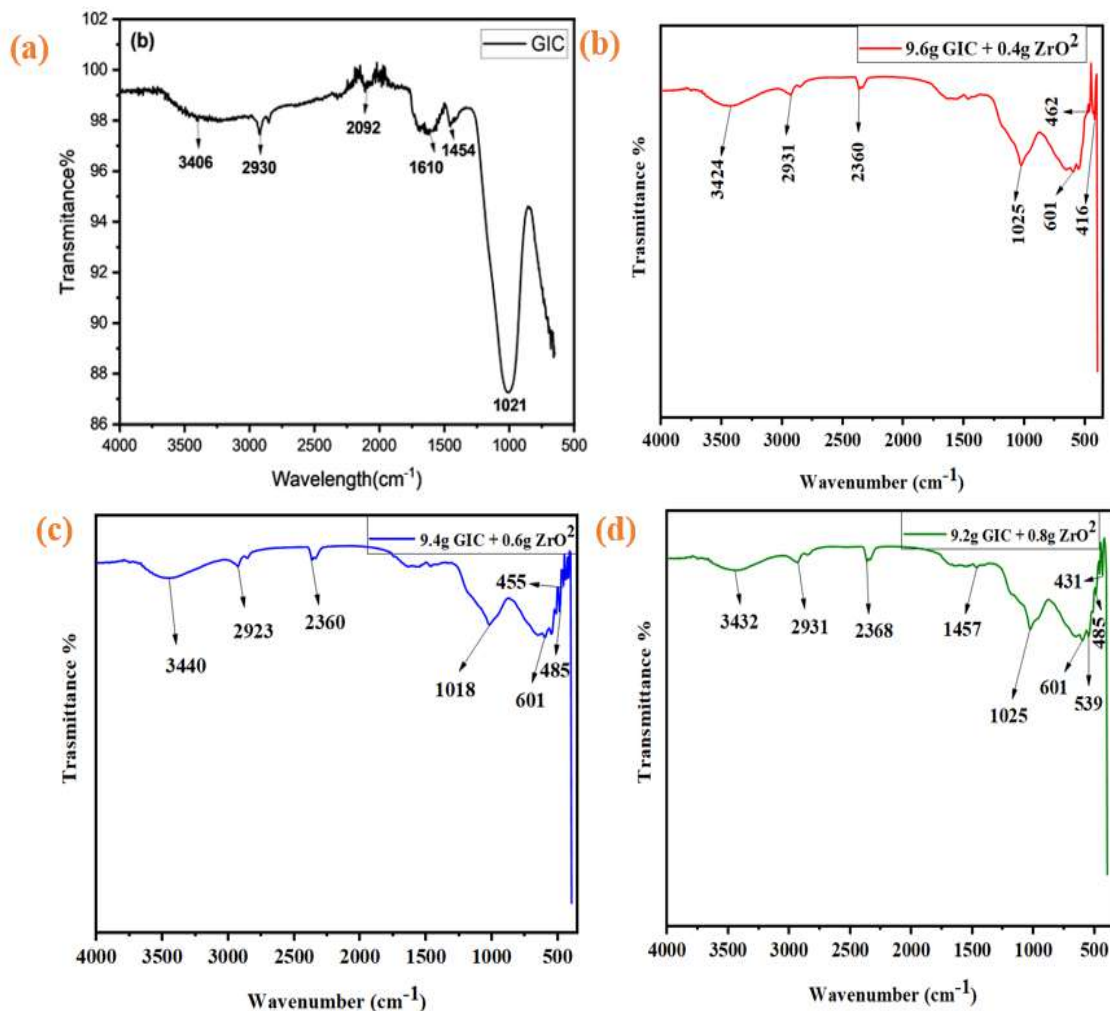


Figure 3.1: FTIR spectra of GIC (a), 4% ZrO_2 + GIC (b), 6% ZrO_2 + GIC (c) and 8% ZrO_2 + GIC (d).

3.2. X-Ray Diffraction Analysis

The crystalline nature of a nano powder of glass ionomer cement was analyzed using an X-Ray Diffractometer with $Cu K\alpha_1$ radiation ($\lambda = 1.54\text{\AA}$). The sample was scanned from $2\theta = 10^\circ$ to 80° at a rate of $0.02^\circ/\text{min}$, with a step size of 0.062 and step time of 0.5s . The XRD pattern of the pure glass ionomer cement showed no distinct peaks, confirming its amorphous character (Moshaverinia et al., 2008).

When zirconium dioxide (ZrO_2) is incorporated into glass ionomer cement (GIC), X-ray diffraction (XRD) analysis typically shows distinct peaks corresponding to the crystalline structure of ZrO_2 . ZrO_2 exhibits characteristic peaks in the XRD pattern that reflect its crystallographic planes and phase composition.

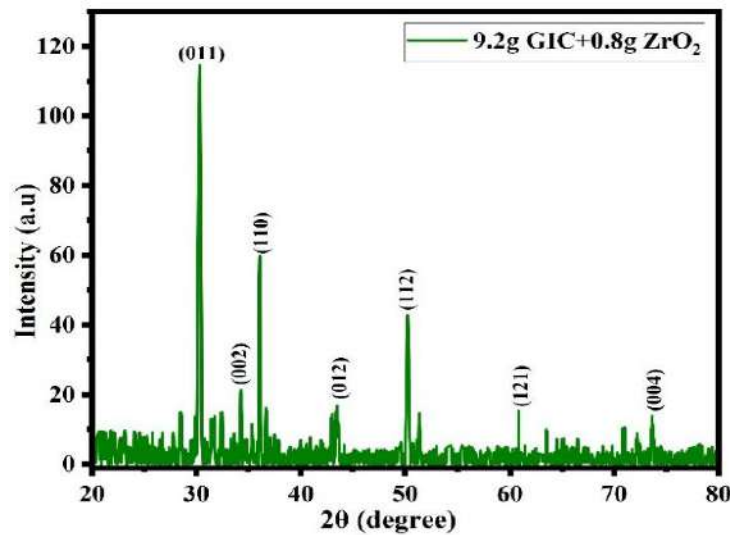
These peaks are sharp and well-defined, indicating the presence of crystalline phases within the GIC matrix. The positions and intensities of these peaks provide valuable information about the distribution, orientation, and quantity of ZrO_2 nanoparticles dispersed in the GIC.

The introduction of epoxy could potentially enhance the material's crystallinity, resulting in more pronounced and well-defined peaks in the XRD pattern compared to the pure GIC (Altaie et al., 2020). The presence of epoxy might also cause shifts in the positions of diffraction peaks in the XRD pattern, indicating alterations in the crystal structure or lattice parameters induced by the epoxy. While some regions of the material may remain amorphous, the XRD analysis could reveal changes

in the degree of amorphousness, with certain areas becoming more crystalline due to the influence of epoxy.

Broad X-ray diffraction halos observed between 30-35° (2θ) indicate the amorphous nature of SiO₂ in commercially available glass ionomer cement (GIC). When epoxy is added, it introduces some crystalline structure to the GIC (Jaman et al., 2021). In X-ray diffraction (XRD) analyses of GICs, distinct peaks often emerge, corresponding to the intercalation of SiO₂ layers within a graphite-like structure, providing insights into the distribution and configuration of SiO₂ within the material.

In the case of zirconium dioxide (ZrO₂), XRD results typically exhibit sharp peaks due to its crystalline nature (Selvam et al., 2013). These peaks correspond to specific crystallographic planes and can reveal information about the crystal structure and purity of ZrO₂ in the GIC composite. Analyzing the positions and intensities of these peaks is crucial for understanding how the addition of ZrO₂ affects the overall structure and properties of the GIC material (Melo et al., 2019).



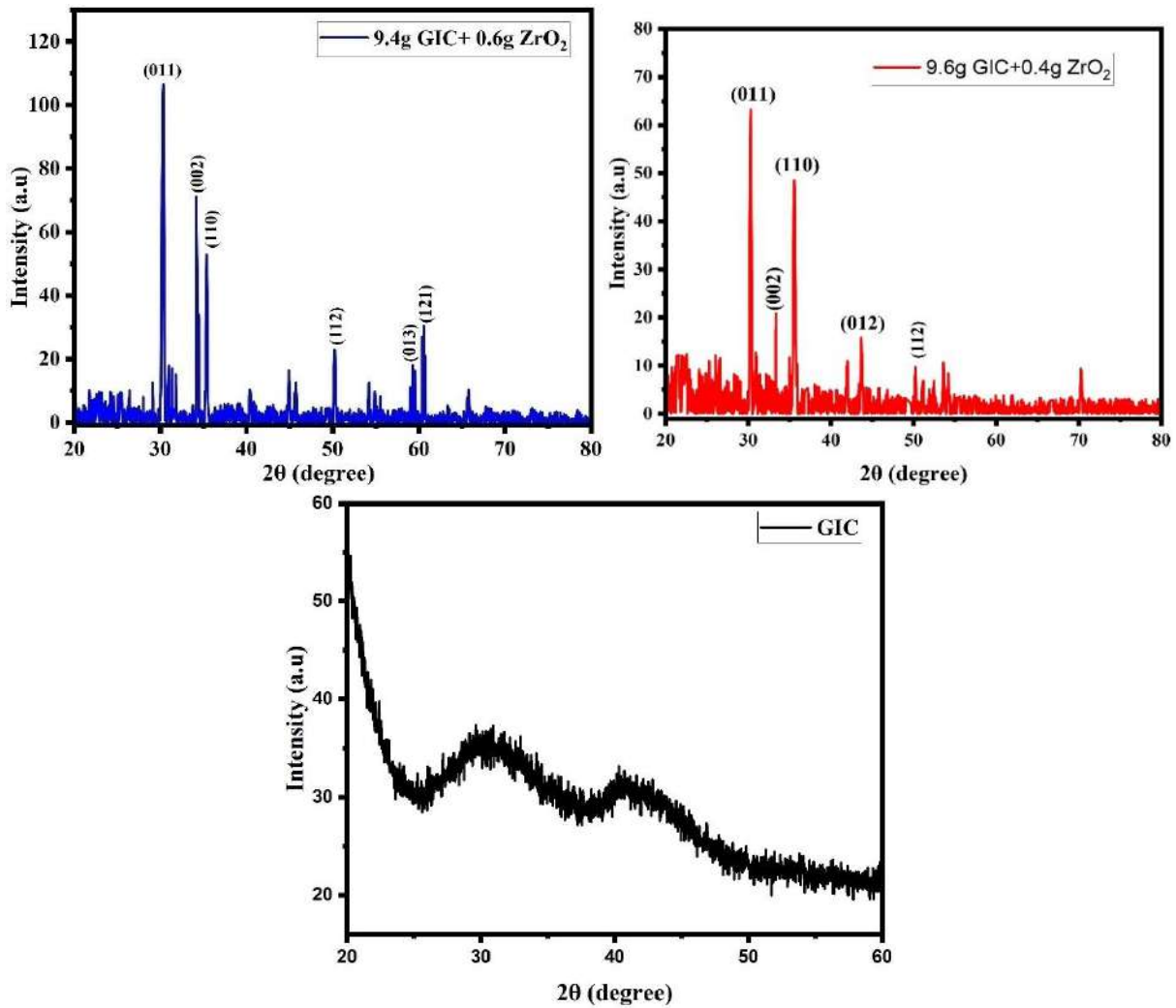


Figure 3.2: XRD patterns for A) Glass ionomer cement (GIC) and ZrO₂ after doping 4%,6% and 8% of: B) 9.6g GIC +0.4g ZrO₂ C) 9.4g GIC +0.6g ZrO₂ and D) 9.2g GIC +0.8g ZrO₂.

3.3. Scanning Electron microscope and Energy Dispersive X-Ray Analysis

The SEM analysis revealed that adding ZrO₂ nanoparticles to GIC notably changes its surface morphology and microstructure (Gjorgievska et al., 2020). The ZrO₂ nanoparticles were evenly distributed and thoroughly incorporated into the

GIC matrix, resulting in a more intricate and refined microstructure with enhanced interfacial bonding. These microstructural improvements are expected to contribute to the observed enhancements in the mechanical properties of the modified GIC.

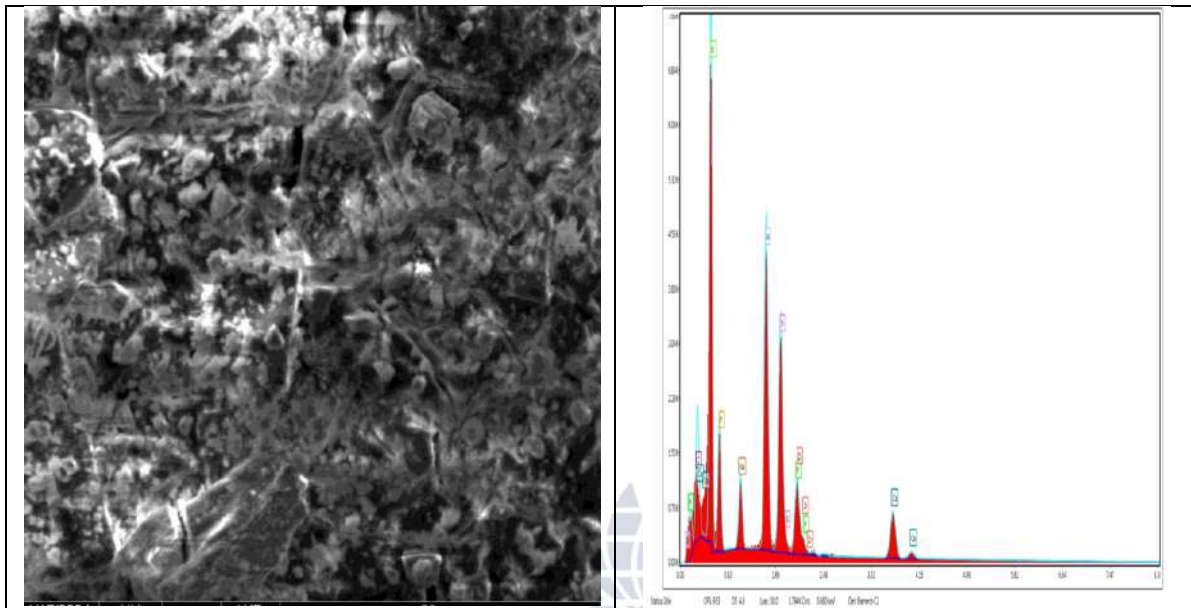


Figure 3.3:SEM and EDX image of 6%wt of ZrO₂ nanoparticle

The EDX analysis of GIC samples with 6% and 8% ZrO₂ nanoparticles revealed comprehensive elemental composition data. For the sample containing 6% ZrO₂, the results confirmed the presence and uniform distribution of zirconium throughout the GIC matrix, indicating successful incorporation of the nanoparticles. Similarly, the sample with 8% ZrO₂ exhibited a higher concentration of zirconium, with a consistent and even dispersion within the GIC. These results affirm the effective integration of ZrO₂ nanoparticles at both concentrations, which likely contributes to the improved mechanical properties observed in the modified GIC.

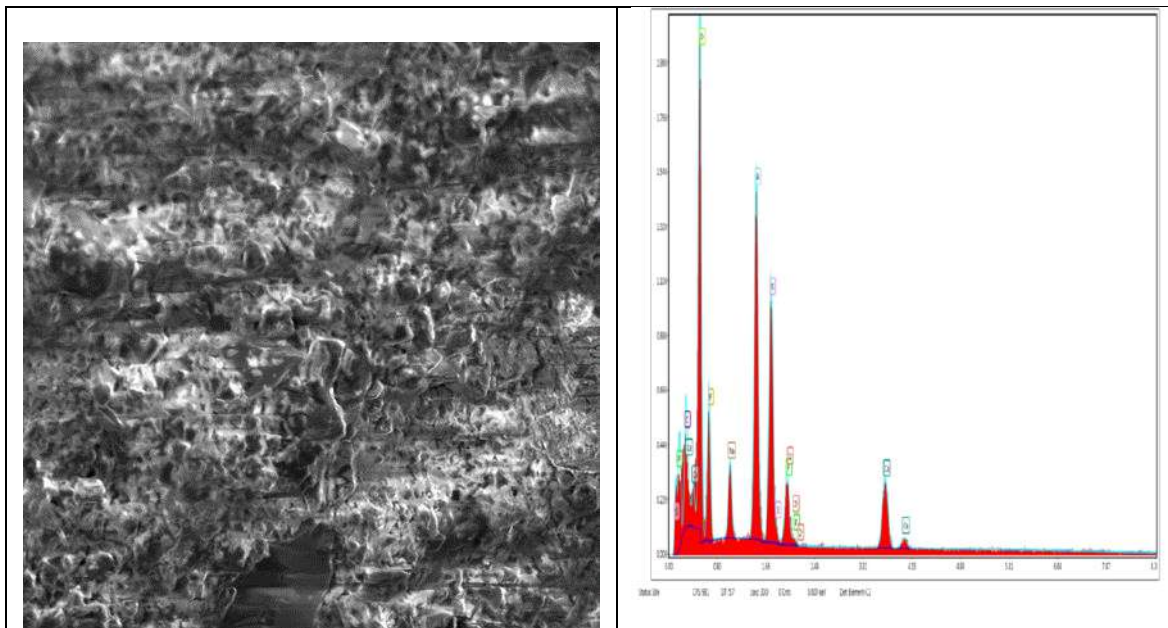


Figure 3.4:SEM image of 8%wt of ZrO2 nanoparticle

Detailed information about the elemental composition of the 8%wt ZrO₂ and GIC is provided in Table 3.3.

Figure 3.4 displays the EDX spectrum, confirming the presence of Zr and O ions. The results exhibit

prominent peaks for O, Al, Si, and Zr each with distinct energy levels. Detailed information about the elemental composition of the 6%wt ZrO₂ and GIC is provided in Table 3.2.

Table 3.2:EDX composition of 6%wt of ZrO₂

Element	Weight %	Atomic %
C K	8.25	14.03
O K	34.31	43.8
Na K	4.37	3.89
Al K	15.51	11.74
Si K	12.42	9.03
P K	3.4	2.24
Zr K	4.34	0.97
Ca K	7.76	3.96
F K	9.64	10.36
Total	100	

Table 3.3:EDX Composition of 8% ZrO₂

Element	Weight %	Atomic %
C K	11.38	23.15
O K	26.61	40.64
Na K	4.6	1.91
Al K	9.37	8.48
Si K	7.43	6.47
Zr K	29.93	8.02
Ca K	8.88	5.42
F K	4.6	5.91
Total	100	

3.4. Mechanical Properties of Glass Ionomer Cement

The mechanical properties of materials are crucial when evaluating their appropriateness for dental restorations. These materials must be capable of withstanding the forces exerted during chewing to function effectively. The durability of a material is influenced by its intrinsic properties and the strength of its atomic bonds, which help maintain stability when exposed to external stresses. Dental restorative materials need to have sufficient strength to endure the complex stresses that occur during the repetitive action of chewing, also known as mastication forces, which typically range from 200 to 400 N.

Dentists and researchers have consistently been concerned about the mechanical performance of dental restorative materials, as their durability is crucial for the long-term success of dental treatments. Various dental restoration materials have been thoroughly studied with respect to their mechanical properties, including tensile strength, fracture toughness, flexural strength, and compressive strength. Recently, there have been several efforts aimed at enhancing the mechanical properties of glass ionomer cements (GICs), with each approach presenting its own benefits and drawbacks. Irie et al. conducted a study where they introduced amalgam, silver, and metal powders into GIC powder as reinforcements. However, this method encountered certain challenges, such as aesthetic concerns and

reduced bonding strength to enamel. When a force is applied to an object, it creates tension within the object and generates a reaction force in the direction opposite to the applied load. Assessing the characteristics of this load can be useful in determining the level of stress experienced by the tested material.

3.5. Tensile Test

Tensile test of specimens were performed by Universal Testing Machine Instron 5966, which is made in the UK. For tensile testing, thin film of 10 g containing the ratio of 4%,6% and 8% was prepared by using ZrO₂ nanoparticles. The prepared thin films were cut in the form of dog bone strips for tensile testing. The detailed results of tensile tests were shown in table. Tensile of 6% wt of ZrO₂ showed the highest Young Modulus at its stress and strain. The addition of ZrO₂ nanoparticles resulted in increased tensile strength, indicating improved resistance to fracture under tension. These findings highlight the potential of ZrO₂-modified GIC to offer superior performance in clinical applications where tensile strength is critical.

Table 3.4: Tensile Test

Sr.No	Concentration	Maximum load [N]	Stress at Maximum Load [MPa]	Strain at Break [%]	Automatic Modulus [MPa]
1	Pure GIC	136.45	13.645	3.7	592
2	GIC+4% ZrO ₂	262.93	15.935	4.4	602.53
3	GIC+6% ZrO ₂	515.32	18.945	5.1	631.39
4	GIC+8% ZrO ₂	530.80	21.0645	5.7	641.33

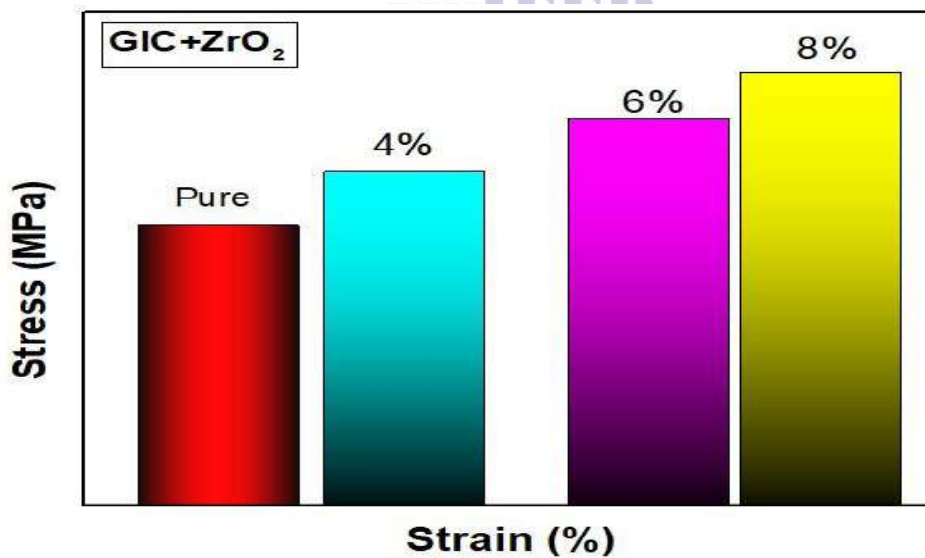


Figure 3.5: Histogram of Stress-Strain

4. Conclusion

The incorporation of ZrO₂ nanoparticles at concentrations of 4%, 6%, and 8% significantly improved the mechanical properties of conventional glass ionomer cement (GIC). The modified composites demonstrated enhanced tensile strength, hardness, and structural stability compared with

unmodified GIC. Among the tested formulations, the sample containing 8% ZrO₂ exhibited the highest Young's modulus, indicating improved stress resistance and mechanical durability. Structural characterization further confirmed the successful integration of ZrO₂ within the GIC matrix,

contributing to improved bonding and material performance. These findings suggest that ZrO₂-reinforced GIC has strong potential for use in restorative dentistry where higher mechanical strength and durability are required. Furthermore, the results highlight the potential of nanoparticle reinforcement for improving dental materials and provide a basis for future studies aimed at optimizing nanoparticle concentration and enhancing additional properties such as biocompatibility and wear resistance.

5. REFERENCES

- Agnihotry, A., Fedorowicz, Z., Nasser, M., Gillies, D., & Hassan, H. (2016). Resin-modified glass ionomer cement versus composite resin for restoring posterior teeth. *Cochrane Database of Systematic Reviews*, (1), CD007744.
- Al-Tae, L. (2019). Secondary caries and restoration replacement: A clinical review. *Journal of Dental Research and Practice*, 13(2), 45–50.
- Altaie, A. S., Hadis, M., & Ellakwa, A. (2020). Influence of nanoparticle incorporation on the mechanical properties of dental restorative materials. *Journal of Prosthodontics*, 29(6), 475–481.
- Chaitra, T. R. (2018). Evaluation of mechanical properties of glass ionomer cements. *Journal of Clinical and Diagnostic Research*, 12(4), ZE01–ZE04.
- Ching, H. S., Luddin, N., Kannan, T. P., Ab Rahman, I., & Abdul Ghani, N. R. (2018). Modification of glass ionomer cements on their physical-mechanical and antimicrobial properties. *Journal of Esthetic and Restorative Dentistry*, 30(6), 557–571.
- Culbertson, B. M. (2001). Glass ionomer dental restorative materials. *Progress in Polymer Science*, 26(4), 577–604.
- de Oliveira, D. C. R. S., Souza, J. Z., & de Menezes, M. (2018). Current restorative materials and minimally invasive dentistry. *International Journal of Dentistry*, 2018, 1–9.
- Ferracane, J. L. (2011). Resin composite—state of the art. *Dental Materials*, 27(1), 29–38.
- Foroughi, F., Hassanzadeh-Tabrizi, S. A., & Saffar-Teluri, A. (2016). Structural and spectroscopic characterization of zirconia nanoparticles. *Ceramics International*, 42(7), 8593–8598.
- Geurtsen, W., Leyhausen, G., & Garcia-Godoy, F. (2003). Effect of dental restorative materials on the tooth-restoration interface. *Clinical Oral Investigations*, 7(2), 71–80.
- Gjorgievska, E., Nicholson, J. W., Slipper, I., & Stevanovic, M. (2020). The influence of nanoparticles on the mechanical properties of glass ionomer cements. *Materials*, 13(12), 2769.
- Goldstein, J., Newbury, D., Joy, D., Lyman, C., Echlin, P., Lifshin, E., Sawyer, L., & Michael, J. (2018). *Scanning electron microscopy and X-ray microanalysis* (4th ed.). Springer.
- Hickel, R., Manhart, J., Garcia-Godoy, F., & Hickel, R. (2007). Clinical results and new developments of direct posterior restorations. *American Journal of Dentistry*, 20(3), 119–123.
- Holland, R. I., & Davis, S. (2008). Degradation of dental composites. *Journal of Dentistry*, 36(12), 968–973.
- Jaman, M. S., Rahman, M. M., & Alam, M. S. (2021). Structural analysis of dental restorative materials using XRD techniques. *Materials Today: Proceedings*, 42, 1215–1219.
- Janssens, K., Van Grieken, R., & Adams, F. (2017). *X-ray spectrometry: Recent technological advances*. Wiley.
- Kahler, W. (2008). The cracked tooth conundrum: Terminology, classification, diagnosis, and management. *American Journal of Dentistry*, 21(5), 275–282.
- Leal, S. C., Abreu, D. M., Frencken, J. E., & Navarro, M. F. L. (2022). Minimally invasive dentistry: The “5Rs” concept for restoration management. *Journal of Dentistry*, 116, 103884.
- Leonard, R. H., & Weber, C. R. (1970). Biofilm and dental caries development. *Journal of Dental Research*, 49(6), 1417–1422.
- Mahla, R. S. (2016). Advances in dental composite materials. *Journal of Advanced Clinical Dentistry*, 7(3), 112–117.

- Melo, M. A. S., Guedes, S. F. F., Xu, H. H. K., & Rodrigues, L. K. A. (2019). Nanotechnology-based restorative materials in dentistry. *Dental Materials*, 35(5), 1-12.
- Meyenberg, K. H. (2013). Replacement versus repair of restorations. *International Journal of Esthetic Dentistry*, 8(1), 56-65.
- Moshaverinia, A., Ansari, S., Movasaghi, Z., Billington, R. W., & Darr, J. A. (2008). Modification of conventional glass ionomer cements with nanoparticles. *Journal of Materials Science: Materials in Medicine*, 19(12), 373-381.
- Mount, G. J., Hume, W. R., Ngo, H., & Wolff, M. (2016). *Preservation and restoration of tooth structure* (3rd ed.). Wiley-Blackwell.
- Nguyen, C., West, N. X., & Joiner, A. (2019). Measurement of dental restorative material hardness. *Journal of Dentistry*, 85, 1-8.
- Nomoto, R., & McCabe, J. F. (2001). Effect of mixing method on the compressive strength of glass ionomer cements. *Journal of Dentistry*, 29(3), 205-210.
- Pani, S. C. (2022). Longevity and failure of dental restorations. *Journal of Conservative Dentistry*, 25(2), 123-128.
- Peres, M. A., Macpherson, L. M. D., Weyant, R. J., Daly, B., Venturelli, R., Mathur, M. R., Listl, S., Celeste, R. K., Guarnizo-Herreno, C. C., & Kearns, C. (2019). Oral diseases: A global public health challenge. *The Lancet*, 394(10194), 249-260.
- Piepenbrock, M. O., Fischer, J., & Dörfer, C. E. (2010). Influence of polyacid modifications on glass ionomer cements. *Dental Materials*, 26(9), 876-884.
- Politis, C., Van Meerbeek, B., & Lambrechts, P. (2016). Longevity of dental restorations: A review. *Clinical Oral Investigations*, 20(2), 251-262.
- Pragathi, A. (2018). Glass ionomer cement in atraumatic restorative treatment. *Journal of Dental Materials and Techniques*, 7(2), 64-70.
- Sahmetlioglu, E., Yilmaz, M., & Arslan, H. (2006). FTIR characterization of zirconium oxide structures. *Spectrochimica Acta Part A*, 65(3-4), 712-716.
- Santos, M. J., & Dahi Taleghani, A. (2022). Glass ionomer cements: A review of their clinical use and performance. *Dental Clinics of North America*, 66(2), 213-230.
- Sarbajna, A., Ghosh, S., & Bera, S. (2017). Influence of tartaric acid on the setting reaction of glass ionomer cement. *Journal of Applied Polymer Science*, 134(23), 44987.
- Selvam, S., Sundrarajan, M., & Kumar, A. (2013). Structural and optical properties of zirconium dioxide nanoparticles. *Ceramics International*, 39(4), 3809-3815.
- Sharif, M. O., Catleugh, M., & Brunton, P. A. (2014). Replacement versus repair of defective restorations: A systematic review. *Journal of Dentistry*, 42(2), 142-151.
- Shurvell, H. F. (2006). Spectra-structure correlation in the mid- and far-infrared. In J. Coates (Ed.), *Encyclopedia of Analytical Chemistry*. Wiley.
- Smith, D. C. (1998). Development of glass ionomer cements. *Biomaterials*, 19(6), 467-478.
- Warren, B. E. (1941). X-ray diffraction methods for determination of crystallite size. *Journal of Applied Physics*, 12(5), 375-384.
- Xie, D., Brantley, W. A., Culbertson, B. M., & Wang, G. (2000). Mechanical properties and microstructures of glass ionomer cements. *Dental Materials*, 16(2), 129-138.